Spring 5-2018

Thiol–Ene Photopolymerization: A Simple Route to Pro-Antimicrobial Networks via Degradable Acetals (PANDAs)

William Martin
University of Southern Mississippi

The University of Southern Mississippi

Thiol–Ene Photopolymerization: A Simple Route to Pro-Antimicrobial Networks via Degradable Acetals (PANDAs)

by

William Blake Martin

A Thesis
Submitted to the Honors College of
The University of Southern Mississippi
in Partial Fulfillment
of the Requirement for the Degree of
Bachelor of Science
in the Department of Polymer Science and Engineering

May 2018

Approved by:

_____

Derek Patton, Ph.D., Thesis Adviser
Department of Polymer Science and Engineering

_____

Jeffrey Wiggins, Ph.D., Chair
Department of Polymer Science and Engineering

_____

Ellen Weinauer, Ph.D, Dean
Honors College

Abstract

The World Health Organization (WHO) has brought the growing epidemic of antibiotic resistance bacteria to the attention of the public and has expressed the need for the development of new methods of defense. In this direction, bioactive aldehyde essential oils have been shown to effectively act as antibiotic and antifungal agents. These bioactive compounds, when used in their pure form, are volatile and lack environmental stability. In this thesis, we describe the synthesis of pro-antimicrobial networks via degradable acetals (PANDAs) using thiol-ene photopolymerization. PANDAs were used as a new model for the high loading and release of bioactive aldehyde-containing compounds via network degradation in response to exposure to acidic pH. Herein, we report the synthesis of diallyl p-chlorobenzaldehyde derived PANDAs to release the antimicrobial form of p-chlorobenzaldehyde under mild conditions (pH 7.4/high humidity).

Keywords: Antibiotic resistance bacteria, essential oils, antimicrobial, thermoset, thio-ene

Dedication

To my family, Bill Martin, Diane Martin, Steven Mitchell, and Gabrielle Mitchell for your endless love and support, without you all I would never have gotten as far as I have. To the two graduate students, Douglas and Dahlia Amato, that have pushed me and motivated me throughout my undergraduate career. Most, if not all, of my success could be traced back to their support, assistance, and motivation. To the undergraduate graduating class of 2017 and 2018, through the countless nights studying together, I have established lifelong friendships and could not have made it through this program without them. Last, but not least, Dr. Patton for giving me the life changing opportunity to work in his lab and providing me with countless opportunities that would not have been achievable.

Acknowledgements

My graduate students, Douglas V. and Dahlia N. Amato; fellow undergraduate researchers, Sarah N. Swilley, Michael J. Sandoz, and Susan B. Walley; our collaborators, the Mavrodi group; and my advisor, Derek L. Patton. The National Science Foundation (OIA-1430364), NSF NRT program "Interface" (DGE-1449999), and Dwaine Braasch for assistance with GC-MS.

Table of Contents

List of Figures and Equations

List of Abbreviations

EOs	Essential Oils
MRSA	Methicillin-resistant *Staphylococcus aureus*
PANDA	Pro-antimicrobial Networks via Degradable Acetals
pCB	Para-chlorobenzaldehyde
pCBA	Para-chlorobenzaldehyde acetal
pTSOH	Para-Toluene Sulfonic Acid
THF	Tetrahydrofuran
TEA	Triethylamine
NMR	Nuclear Magnetic Resonance
SH	Thiol
PETMP	Pentaerythritol Tetra(3-mercaptopropionate)
TTT	1,3,5-triallyl-1,3,5-triazine-2,4,6-trione
RT-FTIR	Real Time-Fourier Transform Infrared
PBS	Phosphate Buffer Solution
MHB	Mueller Hinton II broth
CFU	Colony Forming Units
ZOI	Zone of Inhibition
MHA	Mueller Hinton II Agar
MIC	Minimum Inhibitor Concentration

CHAPTER ONE: INTRODUCTION

Every year, nearly 2 million people are infected with antibiotic resistant bacteria, and of those infected, approximately 23,000 people die as reported by the Center for Disease Control (CDC) in 2013. The threat of drug resistant bacteria will continue to grow annually as antibiotics continue to lose their efficacy. Because of this threat, many efforts have focused on the development and the discovery of alternative methods of defense against these resistant bacteria. Among these efforts, aromatic terpene aldehydes – natural constituents of plant-derived essential oils (EOs) – have been shown to exhibit both antimicrobial and antifungal properties.[1] However, the volatility, chemical instability, and lack of water solubility of aromatic terpene aldehydes have imposed challenges to the development of these materials as effective alternatives and/or supplements to antibiotics derived from pharmaceutical pipelines.[1] In an effort to overcome these challenges, methods such as encapsulation of the EOs within colloidal suspensions or films have been utilized.[1] However, low loading of the EO and uncontrolled burst release profiles observed in these systems eliminate the possibility of controlled, extended release properties necessary for effective antimicrobial applications.

CHAPTER TWO: LITERATURE REVIEW

The 1950s marked the golden age of antibiotics – a period when the discovery of penicillin rapidly accelerated the investigation and development of many other classes of antibiotics.[2-3] However, after World War II, society was threatened by the emergence of penicillin-resistant bacteria arising from the prolific use of antibiotics for the prevention and treatment of bacterial infections.[3] In the early sixties, methicillin was introduced as an effective alternative to penicillin, and within the same decade, methicillin-resistant bacteria

were identified in many patients.[3] Today, the rate of discovery of resistant microbes has vastly exceeded the discovery rate for methods to treat and mitigate these resistant infections.[2]

Among the antibiotic resistant infections, there is not one specific type of bacteria that is shown to be inherently prevalent amongst the human population. Both gram-positive and gram-negative bacteria have developed resistance, and both pose an overall threat.[2] *Staphylococcus aureus* and Enterococcus, examples of gram-positive strains of bacteria, together pose the largest threats to human health and longevity.[2] Methicillin-resistant *Staphylococcus aureus* (MRSA) alone results in more annual human deaths than homicide, AIDS, Parkinson's disease, and emphysema combined.[2] Vancomycin is now employed as a last resort treatment for MRSA. With time and use, vancomycin resistant strains of bacteria have emerged with a mortality rate of 82%.[2] Among the growing threat of antibiotic resistance, gram-negative bacteria have specifically developed a resistance to all available infection treatment options, thus rendering some infections virtually untreatable.[2] *E. coli* results in one of the most common infections, urinary tract infection. As resistant strains of bacteria become more prevalent, then a common treatable infection is likely to become life threatening unless new treatments are discovered. Studies by Andrew Singer have concluded that by the year 2050, resistant microbes will be more prevalent and will cause more deaths annually than cancer.

As bacterial resistance increases, efforts from pharmaceutical and biotechnology companies to develop solutions in this area have lagged. Spellberg et al. examined some of the largest pharmaceutical and biotechnology companies finding that only one new novel antibiotic agent is under development.[4] Thus, to avoid complicated combinatorial synthesis

of new synthetic libraries of compounds, scientists have turned to naturally occurring compounds to combat the growing threat of antibiotic resistance. Among these compounds, plant extracts, or essential oil (EOs), have shown antimicrobial efficacy against these microbes. Since the applications of these EOs have arose, many different applications have been discovered, such as antiviral, antioxidant, and cytotoxic activity.[5-6]

Among the many EOs available, there are different mechanism of action that result in antimicrobial activity. One of the most prominent mechanisms is cell wall disruption – a mechanism observed for tea tree oil.[6] Essential oils are known to contain many polyphenols and terpenoids, which have a high affinity toward proteins and glycoproteins in the cellular membrane, thus enabling high permeation through the cell walls of bacteria.[5] This mechanism of action is also applicable to gram-negative bacteria that have a layer of lipopolysaccharide and protein which reduce the permeability of their membrane relative to gram-positive bacteria.[5] As the EOs permeate through the cell wall causing disruption, the contents within the cell leak leading to bacterial cell death.[5]

However, utilizing EOs on their own poses several challenges such as high volatility, chemical instability and a lack of water solubility.[1] To avert these issues, techniques have been developed to encapsulate EOs to improve their chemical stability and provide controlled release. To obtain exemplary encapsulation, liposomes, coacervation, spray drying, nanoemulsion, nanoprecipitation, nanoparticles, and co-crystallization can be used.[6] However some of these methods, such as liposome encapsulation, have reported encapsulation efficiencies as low as ~ 4%, while also requiring the use of organics solvent that could result in adverse reactions in a biological systems.[6] Other researchers have reported methods, such as nanoparticle encapsulation, that lead to poor release profiles,

yielding only 23% release within 30 days within a pH 7 phosphate buffer solution.[6] Chemical incorporation of the EOs within polymer matrices have shown higher efficiency relative to encapsulation methods.

By chemically incorporating EO into polymers to form a poly(active) network, higher loading and tailored release kinetics can be achieved, overcoming the complications imposed by previous methods of encapsulation.[7] Many polymer systems incorporate the bioactive molecule onto the backbone of the primary polymer used, called the poly(active) approach, and will be released via hydrolysis of the backbone of the polymer.[8-9] As discussed before, this method would cause controlled release of the bioactive, thus preventing the passive burst release that is often provided by encapsulated and conjugated release systems. The degradation rate of these systems can be controlled by the composition of the bioactive molecule linkers that are used within the polymer backbone.[7, 9] However, as the linkers degrade to release the bioactive, the residual polymer backbone ultimately does not undergo biodegradation which will require removal from the system.[7]

In attempt to address the problems associated with EO sequestration, "polyactive" networks can be used. These networks provide high loading of the active therapeutic agents, and through formulation modification, the release rate of the therapeutic agent can be tailored.[7] Other researchers have proposed linear polyactives of phytochemicals as a facile route to provide sustained release of a wide range of pharmaceuticals, such as anti-inflammatories[8, 10], antioxidants[11-12], and anti-cancer compounds.[13-14] While possible, tailoring the rate of release of linear polyactives has its challenges due to the dependence on many parameters, such as crystallinity, molecular weight, functionality and hydrophilicity.[15]

However, polyactive networks provide a more facile route of tailoring the release kinetics by manipulation of the crosslink density, concentration of monomer, and monomer molecular weight.[16] It has recently been shown that biocompatible crosslinked polyactive esters circumvent traditional linear polyactive release control by simple modification of release rates and mechanical properties.[17] While these crosslinked polyester do provide biocompatibility and easier control of degradation rates, polymerization to form these networks take longer than 24 hours at temperature above of 130°C, thus preventing in vivo polymerization. In addition, the degradation of the ester bond results in release of acidic compounds that will lead to a localized decrease in pH, causing an immune response.[18] In attempt to circumvent these challenges, polyactive acetal networks have shown to be a promising alternative due to the mild reaction conditions and pH neutral byproducts.[19]

Herein, we describe the thiol-ene photopolymerization of pro-antimicrobial networks via degradable acetals (PANDAs) from p-chlorobenzaldehyde (pCB). Thiol-ene photopolymerization will allow for rapid and high conversion, minimum oxygen inhibition, and mild reaction conditions, which will circumvent the indicated challenges associated with sequestration of terpene aldehyde.[20] Because of the step-growth activity of thiol-ene photopolymerization, it will be ensured that at every crosslink junction, a degradable pCB-derived acetal. This design will provide full degradation of the thiol-ene network while also providing sustained release of an active antimicrobial compound, pCB, and an inactive degradation byproduct.

CHAPTER THREE: EXPERIMENTAL

Acyclic diallyl *p*-chlorobenzaldehyde acetal (pCBA) was synthesized from *p*-chlorobenzaldehyde (pCB) via acid-catalyzed condensation of pCB with allyl alcohol. Into a flame dried 250ml RBF, 3 Å molecular sieves (15g), pCB (10g, 71.14 mmol, 1 equiv), pTSOH (4.3g, 24.97 mmol, 0.35 equiv), allyl alcohol (16.52g, 284.6 mmol, 4 equiv.), and THF (50 ml). The resulting yellow solution was stirred for 24 hours and quenched via the addition of TEA (19.8 mL, 142.3 mmol, 2 equiv), filtered from the molecular sieves, and the solvent was removed on a rotary evaporator prior to the addition to a silica gel column, eluted with a 1:9 ethyl acetate/hexanes. From the column, 8.3g (48.9%) of pCBA was obtained, and purification verified by ^{1}H NMR on a Varian Mercury Plus 300 MHz NMR in Chloroform-*d* with the following chemical shifts: δ 7.46 (d, J = 8.4 Hz, 1H), 7.36 (d, J = 8.4 Hz, 1H), 5.95 (ddt, J = 16.2, 10.8, 5.6 Hz, 1H), 5.63 (d, J = 2.7 Hz, 1H), 5.33 (dt, J = 17.2, 1.8 Hz, 1H), 5.20 (dd, J = 10.5, 2.1 Hz, 1H), 4.06 (d, J = 5.1 Hz, 2 2H). 13C NMR (75 MHz, CDCl3) δ 136.97, 134.27, 128.41, 128.21, 116.96, 99.63, 66.06.

A solution of pCBA, prepared using the previously described method, was mixed with pentaerythritol tetramercaptopropionate (PETMP) at 1:1 ratio of alkene:SH, with 4 wt.% of the photoinitiator, Darocure 1173, to make 100% loaded PANDA disks. To make 90% loaded PANDA disks, 1,3,5-triallyl-1,3,5-triazine-2,4,6-trione (TTT) was used as another alkene source which contributes to 10% of the total amount of alkene functionality in the system. These mixtures were pipetted onto a glass microscope slide previously treated with Rain-X and containing two Teflon spacers (thickness:0.76 ± 0.02 mm) on both ends of the glass slide. Another Rain-X treated slide was placed onto the first slide, thus

providing an interstitial space to make the PANDA disks. The resulting samples were cured via UV light for 20 minutes using an Omnicure S1000-1B equipped with a 100W mercury lamp (λmax=365 nm, 320-500 nm filter) at an intensity of 200 mW cm^{-2}. Kinetics of polymerization was determined via real-time FTIR with a Nicolet 8700 FTIR spectrometer with a KBr beam splitter and a MCT/A detector with a 320–500 nm filtered ultraviolet light source.

The 25 mm^3 PANDA disks were subsequently placed in a scintillation vial followed by addition of 3 mL of pH 7.4 PBS solution and 15 mL of octanol. The octanol organic layer was used to partition the aldehyde from the aqueous layer, a similar method used by Carter and coworkers. [21] Immediately after addition of the octanol, 100 μL octanol aliquots were removed from the scintillation vials to determine the concentration of the aldehyde. Concentration was determined by measuring the UV-vis absorbance at 275 nm using a BioTek Synergy 2 programmable microplate reader. After measurement of absorbance, the same octanol aliquot was subsequently pipetted back into the corresponding scintillation vials to maintain the same concentration. Aliquots were taken at the following time points: t=0, 20, 24, 30, 48, 54, 72, 78, 102, 120 h. The experiments were performed with n=5, with both the standard deviation and mean reported. After analysis of the concentration over the course of 120 h, the data was then extrapolated from a standard calibration curve.

The antimicrobial activity of the PANDA disks was evaluated via zone of inhibition (ZOI) assay with clinically isolated strains of the following bacteria: *Escherichia coli* (serotype 95 O157:H7), *Staphylococcus aureus* RN6390, *Burkholderia cenocepacia* K56-2, and *Pseudomonas aeruginosa* PAO1. The overlay of the indicator organisms was made by culturing the bacteria in Mueller Hinton II broth (MHB) at 37 °C overnight. From the

overnight cultures, a dilution of 1:5 of cultured MHB and fresh MHB was made, and subsequently mixed with molten soft agar to achieve a CFU concentration of ~10^8 CFU mL^{-1}. The soft agar consisted of the following per liter: 8g of sodium chloride, 10g Bacto Tryptone, and 6g Difco agar. From the mixture of diluted solution and molten soft agar, 4mL was aliquoted onto Mueller Hinton II ager (MHA) plates and allowed to solidify. Once solidified. 25 mm^3 PANDA disks were overlaid on top of the soft agar and incubated at 37 °C. After 30 hours of incubation, the ZOI was measured and reported as the radius from the edge of the PANDA disk to the edge of the ZOI. For each strain, five replicates were conducted and the mean and standard deviation of the ZOI is reported.

The rate of which the 90% pCBA loaded PANDA kill bacteria was conducted via modified terminal dilution method. Two 90% PANDA disks were combined with 3mL of ~10^5 CFU/mL in a test tube. The resulting samples were incubated at 37°C at 200rmp for 30 hours. Six 100µL aliquots of the bacterial suspension was taken at the following time points, after addition of the 90% pCBA loaded PANDA disks: 0, 2, 4, 8, 12, 24, 30 hours. The aliquots were transferred into a 96-well microplate that was prefilled with 200µL of MHB and serially diluted, which it was then incubated for 48hrs at the bacteria's optimal growth temperature. The turbidity of the MHB, after incubation, was measured via BioTek Synergy 2 microplate reader at 600 nm. Optical density ≥0.05 was considered positive for bacterial growth. The number of CFU was calculated by Equation 1, by using the final dilution (TD) that had an optical density of ≥0.05.

$$\frac{CFU}{mL} = \frac{10 \times 3^{TD}}{1\ mL} \quad (1)$$

Minimum inhibitor concentration (MIC) was conducted via a modified broth macrodilution method. PANDA disks ranging from sizes 5-50mm^3 that had between 0.5-

3mg/mL of pCB incorporated into the disk were added to test tubes along with 3 mL of MHB bacterial solution at ~10 CFU mL^{-1}. The resulting samples were then incubated at 37°C at 200rpm for 30 hours. The MHB bacterial solution served as a positive control, whereas the uninoculated MHB was the negative control. Using a BioTek Synergy 2 programmable microplate reader optical density was conducted on the samples at 600nm where an optical density of <0.05 was considered negative for bacterial growth.

A resistance assay was conducted using a similar method described by Haldar and coworkers.[22] The MIC for subsequent studies were conducted by making bacterial solutions from sub-MIC (at MIC/2) of the disks. 3mL of a bacterial solution of ~10^5 CFU/mL, determined via optical density, was pipetted into 3 vials, followed by disks of various sizes. The resulting samples were then incubated for 24 hours, then bacterial solutions were again made using bacteria from the sub-MIC concentrations of the disks. The resistance development was conducted twice, over 20 passages, where the MIC was reported at each passage.

Fungal activity of the 90% loaded pCBA PANDA disks were tested against Trichoderma harzianum and Candida albicans by use of the ZOI method. The fungal cultures were adjusted to OD_{600} 0.1 and 10^5 ppg/mL for C. albicans and T. harzianum, respectfully. From the fungal cultures, 100μL was spread on the surface of Mueller Hinton II (MHA) plates and then a $25mm^3$ disk was placed. These resulting samples were then left to incubate over the course of 72 hours at 30°C.

The cytotoxicity of 90% loaded pCBA PANDA disks were determined via a standard literature procedure.[23] Forty-eight hours prior to the study, the KB cells, from Corning Incorporated, 100μL of 100,000cells/mL was pipetted into a 96 well plate. These

cells were then treated with 50µL of pCB, 50µL of PANDA degradation byproducts, and a 3% DMSO treatment served as a control. A Vybrant MTT Cell Proliferation Kit from Invitrogen was used to determined cell proliferation. Before addition of 10µL of a 12mM MTT reagent to each well of the 96 well plate, the cells were first incubated for 30 hours. For an additional 4 hours, the cells were incubated, for which then the media was removed and replaced by 50µL of DMSO. Cell absorbance was then determined via a Biotek Synergy2 MultiMode Microplate Reader, with a total of four replicates.

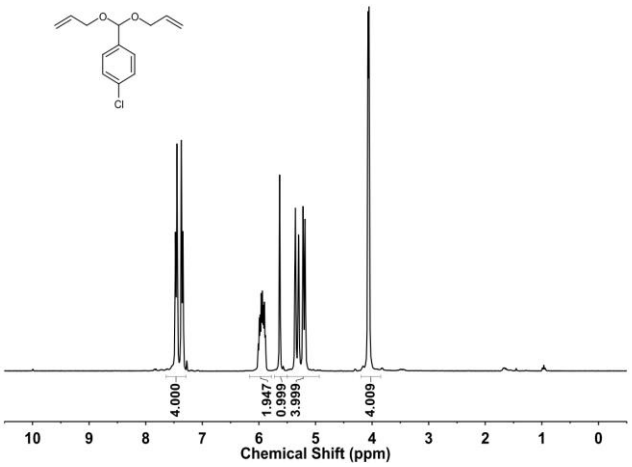

Figure 1. [1] H NMR of diallyl p-chlorobenzaldehyde acetal.

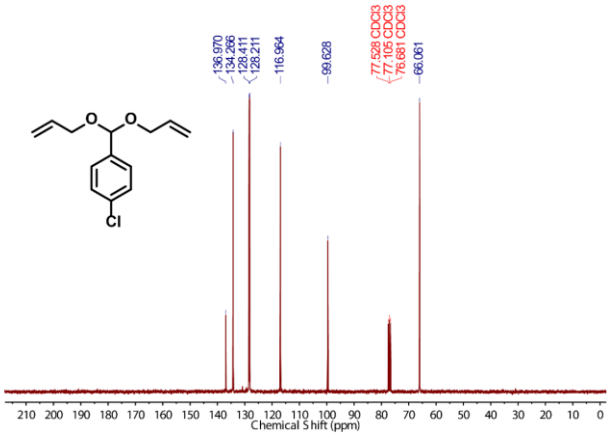

Figure 2. [13]C NMR of diallyl p-chlorobenzaldehyde.

CHAPTER FOUR: RESULTS AND DISCUSSION

The pCBA monomer was successfully synthesized at 49.8% yield via the acid-catalyzed condensation of pCB with allyl alcohol. The structure of the monomer was confirmed via the presence of the acetal proton singlet observed at ~5.5ppm in the [1]H NMR spectrum (Figure 1). The acetal carbon was observed at 99.6 28 ppm by [13]C NMR (Figure 2). The resulting product was then plated against clinically isolated strains of the

following bacteria: *Escherichia coli* (serotype 95 O157:H7), *Staphylococcus aureus* RN6390, *Burkholderia cenocepacia* K56-2, and *Pseudomonas aeruginosa* PAO1. The resulting pure pCBA exhibited no antibacterial properties due to the lack of an unprotected aldehyde, thus no ZOI is observed, even at the highest tested concentration of 10mg/mL. The degradation product, pCB, showed significant antibacterial properties, even at 0.5mg/mL. From this data, it shows that the acylic acetal serves as a pro-antimicrobial compound, meaning that antibacterial efficacy is provided upon degradation into an aldehyde.

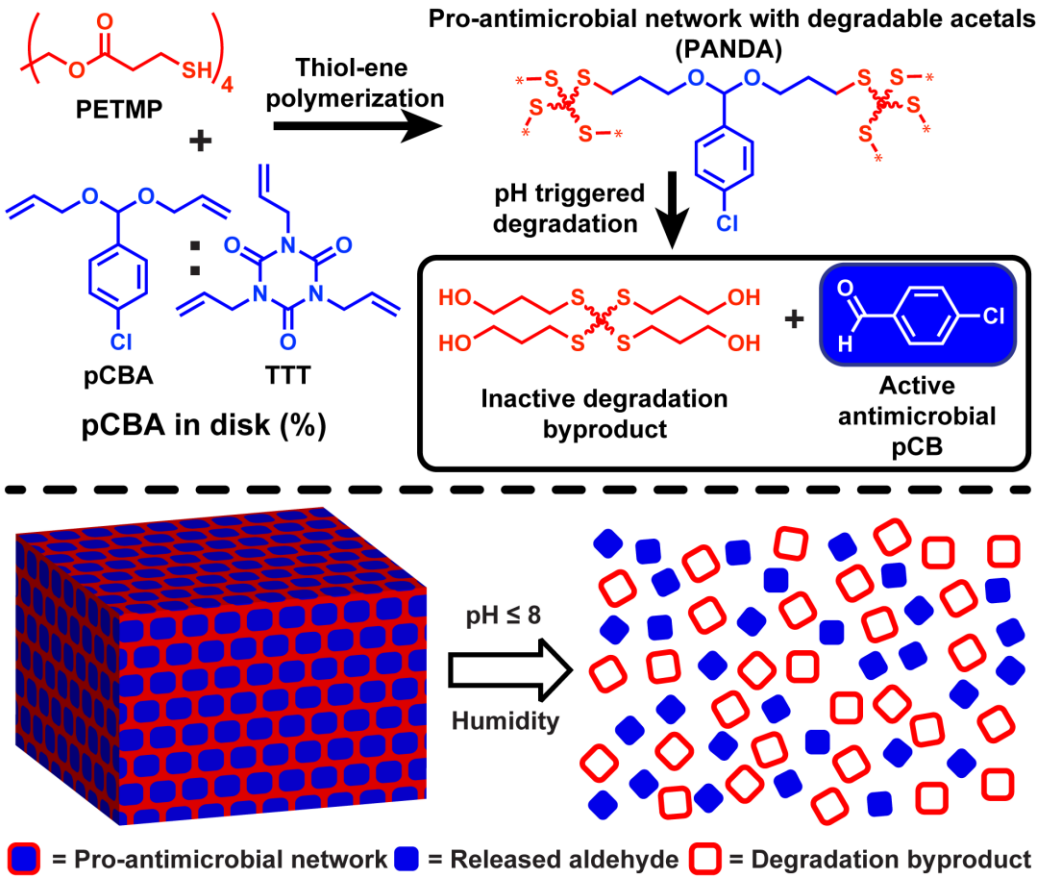

Scheme 1. Synthesis of PANDAs and major degradation byproducts.

UV-curable PANDA resins were then formulated with a photoinitiator, pentaerythritol tetramercaptopropionate (PETMP), and varied concentrations of pCBA relative to non-degradable 1,3,5-triallyl-1,3,5-triazine-2,4,6-trione (TTT) with 1:1

alkene:thiol mole stoichiometry (Scheme 1). According to Scheme 1, PANDAs are molecularly designed to undergo complete degradation upon hydrolysis resulting in the release of pCB as an active antimicrobial and antifungal agent, and the generation of inactive low molecular weight degradation byproducts. The UV-photopolymerization of PANDA disks from the 9:1 pCBA:TTT formulation resulted in transparent, low modulus thermosets with a T_g of 0.5°C, as determined via dynamic mechanical analysis (Figure 3b). The kinetics of this polymerization yielded rapid and high conversion of both the alkene and thiol group, as determined via RT-FTIR (Figure 3a). Through altering of the feed ratio of TTT to pCBA, different mechanical properties can be seen, such as difference in flexibility, degradation, and Tg.

To explore the release of pCB from the 25 mm^3 PANDA films, we submerged the films in solutions consisting of two phases – an organic phase (octanol) and an aqueous phase (PBS, pH 7.4 and pH 6.0). The organic phase was used to partition the aldehyde from the aqueous layer. Aliquots from the organic phase over time were analyzed via UV-vis spectroscopy to determine release as a function of time. Figure 3c shows the release kinetics of the 90% loaded pCBA PANDA disks for pH 7.4 and 6.0 over 120 hours. A lag time of ~20 hours can be seen at both tested pH values before pCB begins to release from the degradable linkages within the polymer network, where 14% (1.07 mg/mL) and 53% (4.19 mg/mL) at 24 and 48 hours, respectively at pH 7.4 and similar release at pH 6.0. However, by 120 hours, only 72% release was observed at pH 7.4, whereas at pH 6.0 a higher release occurred (80%). The higher release at lowered pH is due to the relative instability of the acylic acetal against low pH. However, because of this lack of stability to acidic environment, the hydrolysis of the acetal should be proportional to the concentration

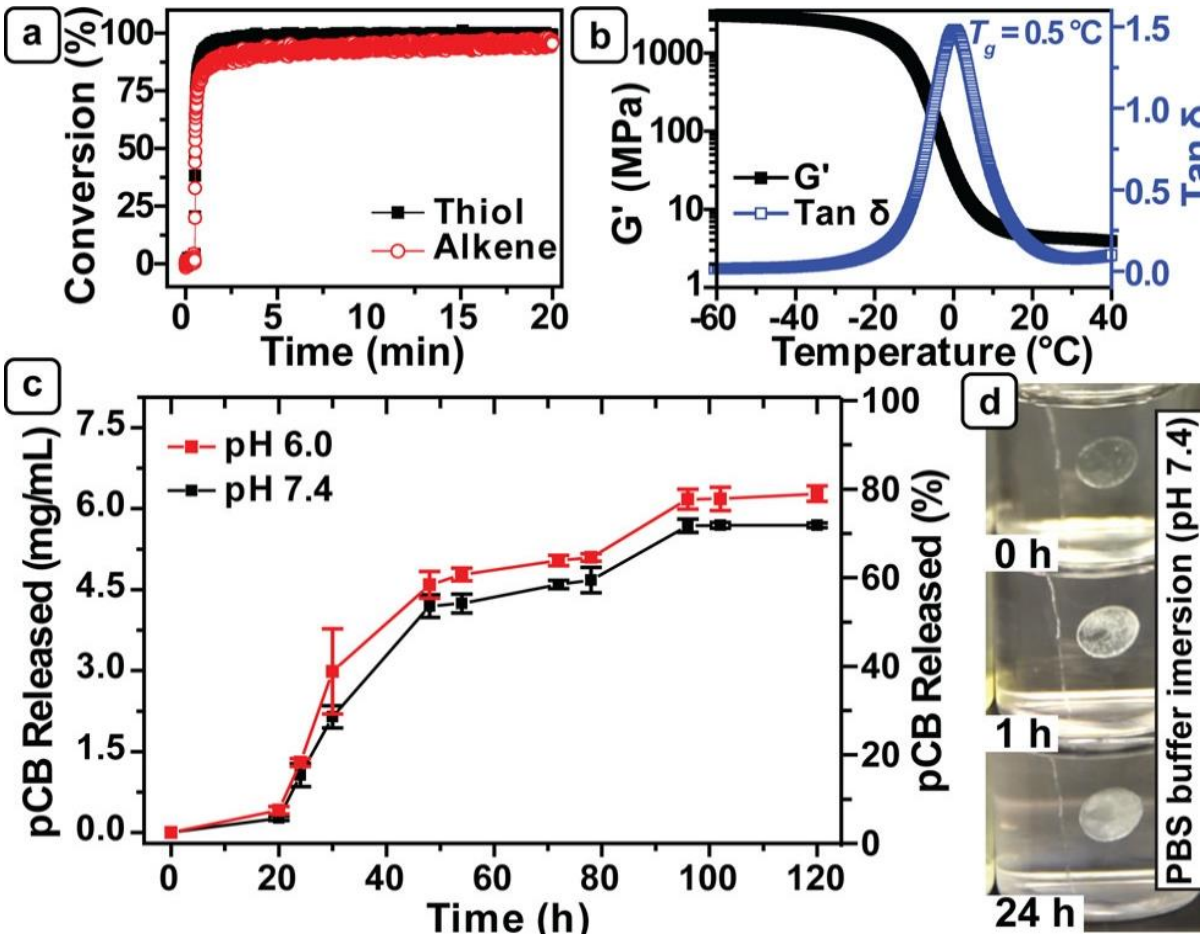

Figure 3. RT-FTIR cure kinetics, DMA, pCB release kinetics, and degradation behavior of 90% loaded pCBA PANDA disks. (a) UV Conversion kinetics at cured at an intensity 200mW/cm^2. (b) Representative thermomechanical plot. (c) pCB release at pH 6.0 and 7.4 in octanol/PBS. (d) PANDA degradation time-lapse characterized via optical microscopy.

of hydronium ions in the solution used rather than a simple increase in degradation kinetics. This phenomena is attributed to the surface erosion behavior of the PANDA disks caused by incorporation of pCBA into a hydrophobic network.[24]

The PANDA disks should exhibit surface erosion behavior when characterized by optical microscopy. In the photo series of Figure 3d, 25 mm^3 PANDA disks were submerged in pH 7.4 PBS and monitored over time. By 1 hour, the surface of the PANDA disk changed from translucent to opaque. At 24 hours, the PANDA disk shrank in size but retained its shape, thus verifying surface erosion behavior. The observed surface erosion

behavior is typical of polyacetals and expected due to the hydrophobicity of the polymer disks, as seen by its contact angle of ~90°.

PANDAs were designed for end-use as potential applications where antimicrobial material is needed. Using ZOI experiments, the efficacy of the PANDA material was evaluated against the following bacteria: *Escherichia coli* (serotype 95 O157:H7), Staphylococcus aureus RN6390, *Burkholderia cenocepacia* K56-2, and *Pseudomonas aeruginosa* PAO1. As shown in Figure 4a, the control PANDA disk, containing 0% loading of pCBA, resulted in no zone of inhibition which is used as a negative control. Using pCBA loadings from 60% to 100%, relative to TTT, showed that with increasing loading of the pCBA a larger ZOI was observed. When >90%, the ZOI was seen to remain constant, thus any subsequent antimicrobial studies were conducted using 90% pCBA loaded PANDA disks. The efficacy of the material was further analyzed via terminal dilution assay to determine kill kinetics (Figure 4b). Two 25 mm^3 90% loaded pCBA PANDA disks showed >5 log decrease in bacteria count in <12 hours, resulting in kill efficiencies of >99.999%.

To evaluate whether bacteria developed resistance to pCB, a resistance assay was conducted and compared to the resistance assay of the commercially available antibiotic, Tetracycline, against *P. aeruginosa* using serial passage mutagenesis assay. Figure 4c shows the fold increase in MIC as a function of serial passages, and by the 20^{th} passage, the MIC for tetracycline nearly increased 10-fold, whereas the MIC for pCB remains constant over 20 passages. Because there is no fold increase observed for the MIC of pCB, P. aeruginosa is less likely to develop resistance, thus making this a practical method of hindering the development and spreading of resistance bacteria.

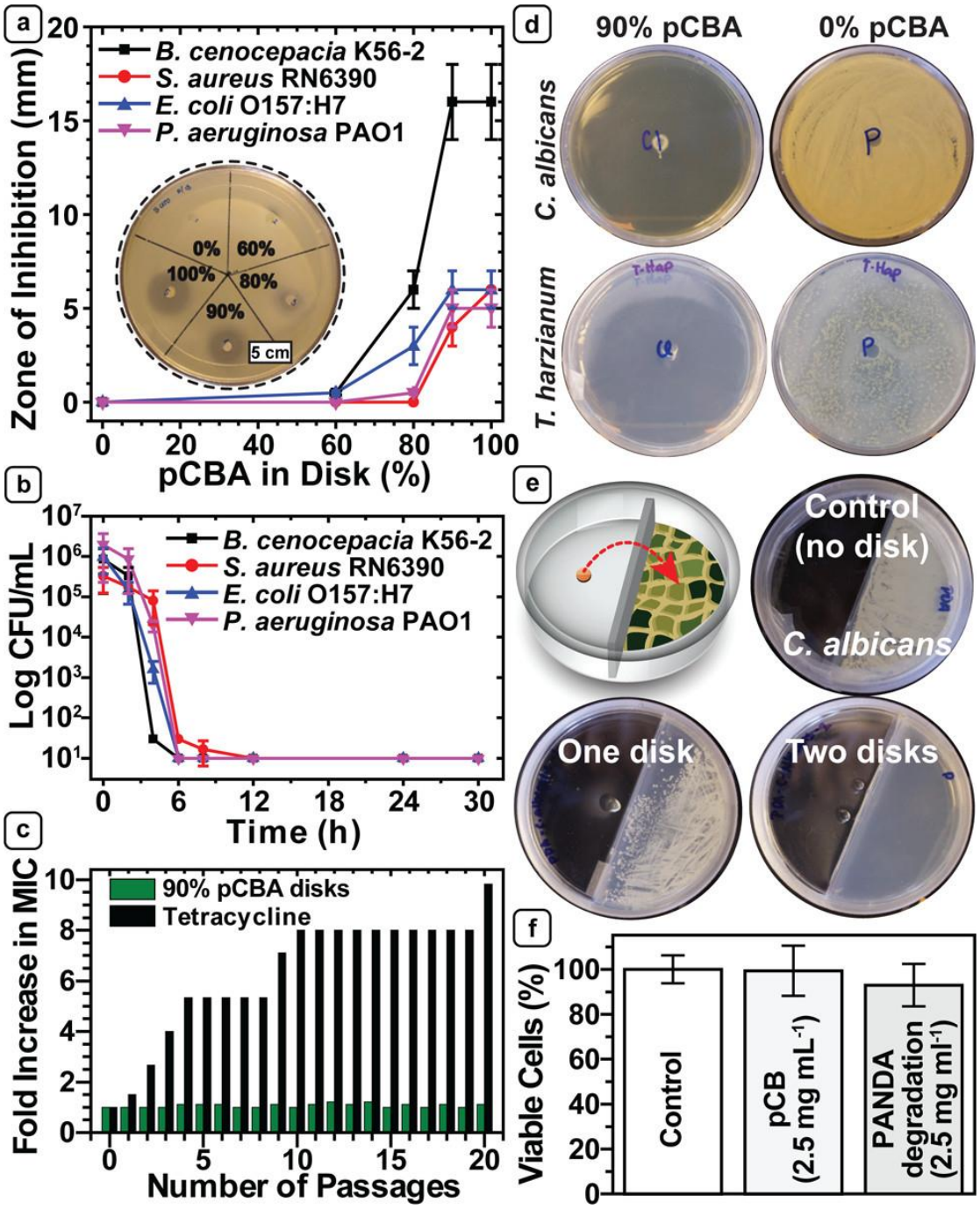

Figure 3. ZOI assay, Kill kinetics, Resistance Assay, Antifungal property analysis, Split plate diffusion assay, Cytotoxcicity assay of 90% loaded pCBA PANDA disks. (a) ZOI assay to show ZOI as a function of percent loading of pCBA. (b) Kill kinetics of four representative bacteria via terminal dilution assay. (c) Resistance assay of 90% loaded pCBA PANDA disks and tetracycline against *P. aeruginosa*. (d) ZOI diffusion assay of 0% and 90% loaded pCBA PANDA disks against *T. harzianum* and C. albicans. (e) Split plate diffusion assay against C. albicans over 90 days. (f) Cytotoxicity assay with 2% DMSO, pCB, and degraded 90% loaded pCBA PANDA disk.

The antifungal properties of 25 mm^3 90% loaded pCBA PANDA disks were determined via ZOI against C. albicans and T. harizianum. As seen in Figure 4d, complete inhibition of growth of both tested fungi was observed by the placement of 1 PANDA disk onto the agar with platted fungi. The 0% loaded pCBA PANDA disk yielded no inhibition of growth, thus the antifungal properties are exclusive to pCB. Knowing the volatility of pCB, a split plate inhibition volatility assay was used to inhibit the growth of C. albicans without contacting the PANDA material. A petri dish with a partition was used and on one side, C. albicans was plated, and on the opposite side a 25 mm^3 90% loaded pCBA PANDA disk was plated. The petri dish was sealed and allowed to incubate for 30 days. Through using one disk, only partial growth inhibition was observed, whereas when two was used complete inhibition was observed (Figure 4e). As expected, 0% loaded pCBA PANDA disk did not exhibit any inhibition of growth. Cytotoxicity of the PANDA material was determined by using a model cell line and incubating the cells with the material. The chosen cell line was KB cells which are derived from a glandular cancer of the cervix. These cells were incubated in an aqueous solution containing a 90% loaded pCBA PANDA disk that has been left to degrade for 7 days at pH 7.4, releasing 2.5 mg/mL pCB. Another solution was used to incubate the cells and consisted of just pCB at 2.5mg/mL, and a control. As seen from Figure 4f, there is no notable toxicity because the cell viability was maintained above 90% observed, thus the material shows promise of possible biocompatibility.

In conclusion, we have successfully designed pro-antimicrobial networks via degradable acetals. This material undergoes degradation in exposure to solutions of pH <8 and in atmosphere of mild humidity to release a bioactive compound that serves as a potent and highly efficient antimicrobial agent against both fungi and bacteria. The released

benzaldehyde as well as the other degradation byproducts exhibit high cytocompatibility, thus allowing for future applications in the biomedical and food industries. We have also demonstrated growth inhibition of *C. albicans* utilizing the volatility of essential oils, eliminating the need for the material to be in direct contact with the fungi. Most importantly, *P. aeruginosa* was unable to develop resistance to pCB in 20 serial passages, whereas resistance was quickly developed toward the commercially available antibiotic, tetracycline.

References

1. Amato, D. N.; Amato, D. V.; Mavrodi, O. V.; Martin, W. B.; Swilley, S. N.; Parsons, K. H.; Mavrodi, D. V.; Patton, D. L., Pro-Antimicrobial Networks via Degradable Acetals (PANDAs) Using Thiol–Ene Photopolymerization. *ACS Macro Letters* **2017,** *6* (2), 171-175.
2. Conly, J. M.; Johnston, B. L., Where are all the new antibiotics? The new antibiotic paradox. *The Canadian Journal of Infectious Diseases & Medical Microbiology* **2005,** *16* (3), 159-160.
3. Ventola, C. L., The Antibiotic Resistance Crisis: Part 1: Causes and Threats. *Pharmacy and Therapeutics* **2015,** *40* (4), 277-283.
4. Spellberg, B.; Powers, J. H.; Brass, E. P.; Miller, L. G.; Edwards, J. J. E., Trends in Antimicrobial Drug Development: Implications for the Future. *Clin. Infect. Dis.* **2004,** *38* (9), 1279-1286.
5. Yap, P. S. X.; Yiap, B. C.; Ping, H. C.; Lim, S. H. E., Essential Oils, A New Horizon in Combating Bacterial Antibiotic Resistance. *The Open Microbiology Journal* **2014,** *8*, 6-14.
6. Dorman, H. J. D.; Deans, S. G., Antimicrobial agents from plants: antibacterial activity of plant volatile oils. *Journal of Applied Microbiology* **2000,** *88* (2), 308-316.
7. Stebbins, N. D.; Faig, J. J.; Yu, W.; Guliyev, R.; Uhrich, K. E., PolyActives: Controlled and Sustained Bioactive Release Via Hydrolytic Degradation. *Biomaterials science* **2015,** *3* (8), 1171-1187.
8. Carbone-Howell, A. L.; Stebbins, N. D.; Uhrich, K. E., Poly(anhydride-esters) Comprised Exclusively of Naturally Occurring Antimicrobials and EDTA: Antioxidant and Antibacterial Activities. *Biomacromolecules* **2014,** *15* (5), 1889-1895.
9. Larson, N.; Ghandehari, H., Polymeric Conjugates for Drug Delivery. *Chemistry of Materials* **2012,** *24* (5), 840-853.
10. Bien-Aime, S.; Yu, W.; Uhrich, K. E., Pinosylvin-Based Polymers: Biodegradable Poly(Anhydride-Esters) for Extended Release of Antibacterial Pinosylvin. *Macromol. Biosci.* **2016,** *16* (7), 978.
11. Ouimet, M. A.; Griffin, J.; Carbone-Howell, A. L.; Wu, W. H.; Stebbins, N. D.; Di, R.; Uhrich, K. E., Biodegradable Ferulic Acid-Containing Poly(anhydride-ester):

Degradation products with Controlled Release and Sustained Antioxidant Activity. *Biomacromolecules* **2013,** *14* (3), 854.
12. Ko, E.; Jeong, D.; Kim, J.; Park, S.; Khang, G.; Lee, D., Antioxidant Polymeric Prodrug Microparticles as a Therapeutic System for Acute Liver Failure. *Biomaterials* **2014,** *35* (12), 3895.
13. Lv, L.; Guo, Y.; Shen, Y.; Liu, J.; Zhang, W.; Zhou, D.; Guo, S., Intracellularly Degradable, Self-Assembled Amphiphilic Block Copolycurcumin Nanoparticles for Efficient In Vivo Cancer Chemotherapy. *Adv. Healthcare Mater.* **2015,** *4* (10), 1496.
14. Kim, B.; Lee, E.; Kim, Y.; Park, S.; Khang, G.; Lee, D., Dual Acid-Responsive Micelle-Forming Anticancer Polymers as New Anticancer Therapeutics. *Adv. Funct. Mater.* **2013,** *23* (40), 5091.
15. Burkoth, A.; Burdick, J.; Anseth, K., Surface and Bulk Modifications to Photocrosslinked Polyanhydrides to Control Degradation Behavior. *J. Biomed. Mater. Res.* **2000,** *51* (3), 352.
16. Rydholm, A. E.; Reddy, S. K.; Anseth, K. S.; Bowman, C. N., Controlling Network Structure in Degradable Thiol−Acrylate Biomaterials to Tune Mass Loss Behavior. *Biomacromolecules* **2006,** *7* (10), 2827-2836.
17. Chandorkar, Y.; Bhagat, R. K.; Madras, G.; Basu, B., Cross-Linked, Biodegradable, Cytocompatible Salicylic Acid Based Polyesters for Localized, Sustained Delivery of Salicylic Acid: An In Vitro Study. *Biomacromolecules* **2014,** *15* (3), 863.
18. Lu, L.; Peter, S. J.; D. Lyman, M.; Lai, H. L.; Leite, S. M.; Tamada, J. A.; Uyama, S.; Vacanti, J. P.; Robert, L.; Mikos, A. G., In vitro and In vivo Degradation of Porous Poly(dl-lactic-co-glycolic acid) Foams. *Biomaterials* **2000,** *21* (18), 1837.
19. Binauld, S.; Stenzel, M. H., Acid-degradable Polymers for Drug Delivery: A Decade of Innovation. *Chem. Commun.* **2013,** *49* (21), 2082.
20. Hoyle, C. E.; Bowman, C. N., Thiol–Ene Click Chemistry. *Angew. Chem., Int. Ed.* **2010,** *49* (9), 1540.
21. Kim, S.; Linker, O.; Garth, K.; Carter, K. R., Degradation Kinetics of Acid-Sensitive Hydrogels. *Polym. Degrad. Stab.* **2015,** *121*, 303.
22. Yarlagadda, V.; Samaddar, S.; Paramanandham, K.; Shome, B. R.; Haldar, J., Membrane Disruption and Enhanced Inhibition of Cell‐Wall Biosynthesis: A Synergistic Approach to Tackle Vancomycin‐Resistant Bacteria. *Angewandte Chemie International Edition* **2015,** *54* (46), 13644-13649.
23. Riss, T. L. M., R. A.; Niles, A. L.; Benink, H. A.; Worzella, T. J.; Minor, L., Cell Viability assays. *Assay Guidance Manual* **2015**.
24. Fife, T. H.; Jao, L. K., Substituent Effects in Acetal Hydrolysis. *J. Org. Chem.* **1965,** *30* (5), 1492.